

Fermi-LAT data reprocessed with updated calibration constants

J. Bregeon

INFN-Sezione di Pisa, Largo Pontecorvo 3, Pisa, I-56127, Italy

E. Charles, M. Wood

KIPAC and SLAC National Accelerator Laboratory, Menlo Park, CA, USA

for the Fermi-LAT collaboration

Four years into the mission, the understanding of the performance of the *Fermi* Large Area Telescope (LAT) and data analysis have increased enormously since launch. Thanks to a careful analysis of flight data, we were able to trace back some of the most significant sources of systematic uncertainties to using non-optimal calibration constants for some of the detectors. In this paper we report on a major effort within the LAT Collaboration to update these constants, to use them to reprocess the first four years of raw data, and to investigate the improvements observed for low- and high-level analysis. The Pass 7 reprocessed data, also known as P7REP data, are still being validated against the original Pass 7 (P7) data by the LAT Collaboration and should be made public, along with the corresponding instrument response functions, in the spring of 2013.

1. Fermi-LAT calibration constants

The *Fermi*-LAT data acquisition system electronics relies on a number of calibration constants (we refer the reader to Abdo et al. [2009] for more details). Most of them are either stable or drift very slowly ($\sim 1\%$ per year). We keep track of the calibration constants for a definite time span with a dedicated database.

For the Anticoincidence Detector (ACD) subsystem, pedestals, low- and high-range gains need to be calibrated. For the Tracker (TKR) subsystem, hot and dead strips have to be identified and the time-over-threshold charge scale must be defined. For the Calorimeter (CAL) subsystem, pedestals, gains, electronics non-linearity and cross-talk are measured through periodic triggers and charge injection runs. In addition, two intrinsic characteristics of the CAL CsI(Tl) crystals must be calibrated: the light yield and the light tapering. We note in passing that other calibrations, such as the alignment of the TKR, appear to have changed negligibly over the mission to date.

The calibration constants used for the P7REP data caused two significant changes with respect to the P7 data: a slight shift in the LAT energy scale, and an improvement the shower imaging resolution of the CAL.

1.1. Energy scale

On-orbit, we measure the CsI(Tl) light yield by selecting minimum ionizing protons from the LAT triggers. The calorimeter CsI(Tl) crystals suffer radiation damage, which induces a decrease of the scintillation efficiency by $\sim 1\%$ per year as shown in figure 1. P7REP data benefited from up-to-date calibration constants for the CsI(Tl) light yield.

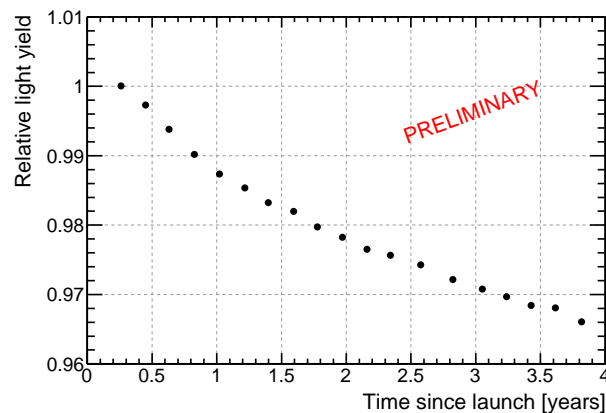


Figure 1: Relative variation of the absolute energy scale, as measured from the pathlength-corrected energy deposition of on-orbit minimum ionizing protons, throughout the first four years of the mission.

1.2. Light asymmetry

The attenuation of light along the longitudinal axis of each CsI(Tl) crystal has to be calibrated on a regular basis as the light asymmetry between the two crystal ends is used to reconstruct the longitudinal position of the energy deposit. The calibration is performed using cosmic-ray heavy ions that release their energy only via ionization: heavy ions provide well localized high-energy depositions, very suitable for this purpose. As we have learned since launch, the measurement of light asymmetry has a direct and significant impact on the determination of the energy centroid in the calorimeter, which is used in the tracking stage of the event reconstruction. This, in turn, determines the instrument point-spread function (PSF). P7REP data were processed with light tapering calibration updated every 2 months.

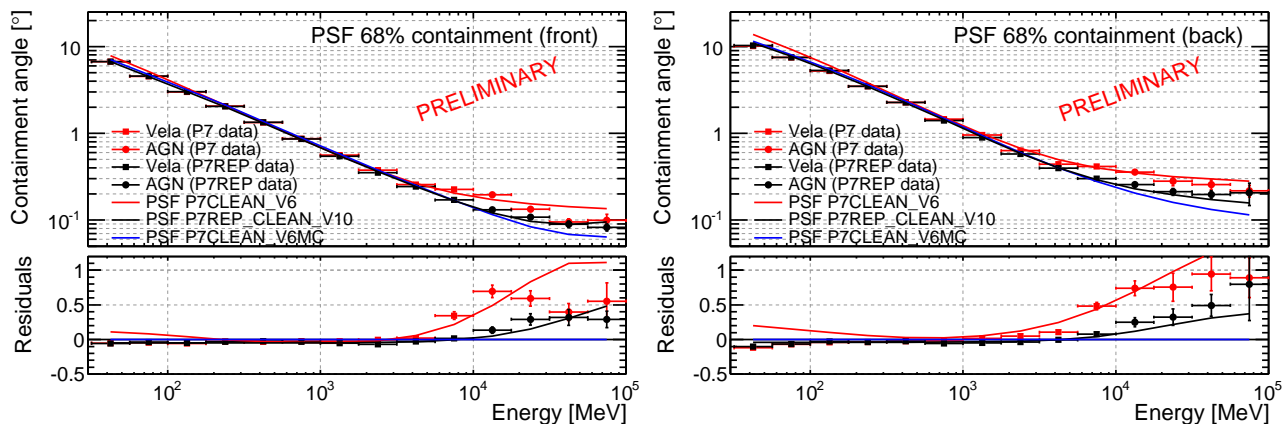


Figure 2: PSF 68% containment radii for front- and back-converting events, derived from on-orbit data (using the Vela pulsar and a stacked sample of AGN) for both P7CLEAN and P7REP_CLEAN. The solid lines show the PSF parameterizations for the P7CLEAN_V6MC, P7CLEAN_V6 and P7REP_CLEAN_V10 sets of IRFs.

2. Instrument Response Functions

The analysis of *Fermi*-LAT data requires a number of tools and ancillary data products including templates for the isotropic and Galactic diffuse emission and instrument response functions (IRFs). All components will be updated to match the characteristics of P7REP data and will be released together with the P7REP data for the purpose of improved data analysis. A preliminary set of IRFs have been produced to match the P7REP data and have been labeled P7REP_V10, e.g., P7REP_SOURCE_V10. As the various analysis components are still being validated, we anticipate that the results shown here may change slightly by the time the P7REP data are released. The corresponding IRFs likewise would be a later iteration (e.g., P7REP_V12 or P7REP_V13) with changes in the effective area at the $\sim 5\%$ level with respect to the P7REP_V10 IRFs presented here. The *Fermi* Science Support Center (FSSC)¹ is the authoritative source for recommendations regarding the analysis of *Fermi* data.

The P7REP_V10 IRFs include our best understanding of the instrument. As for the P7_V6 version available now, they were derived for the event classes used in standard LAT data analysis and for the tracker thin-converter section (front) and thick-converter section (back) separately (see Ackermann et al. [2012] for more details). The P7REP_V10 IRFs have been derived as usual using GEANT4-based [Agostinelli et al. 2003] MC simulations. However, both the effective area and the PSF have been refined using information from flight data.

For the effective area, analysis of photons from the

Vela pulsar and the Galactic Ridge have shown that, when analyzed separately, front- and back-converting events give inconsistent results for the absolute measured flux. The observed discrepancy is very likely due to differences between the true and simulated instrument response and has been a long-standing issue observed since launch. Because we cannot determine from flight data whether the front or back response is more accurate, we applied a symmetric correction factor to both in order to keep the total front + back effective area unchanged. The front/back ratio discrepancy ranges from -8% at 100 MeV to $+4\%$ at 300 MeV and greater.

For the PSF, we analyzed P7REP_CLEAN event-class data from the Vela pulsar and a sample of 40 bright active Galactic nuclei (AGN) and found a significant improvement in pointing resolution above 1 GeV with respect to non-reprocessed data. Because the on-orbit PSF is now much closer to the MC-derived PSF, we developed a new method to parameterize the former. We have generated an on-orbit PSF model for P7REP using the same King-function parameter tables as the MC-derived PSF P7CLEAN_V6MC but with different coefficients for the PSF scaling function, which are fit to match the PSF distributions of the Vela pulsar and AGN calibration data sets. We find that the PSF of P7REP_CLEAN_V10 is significantly improved relative to P7 with a 30% (40%) reduction in the PSF 68% containment radius for front (back) events above 10 GeV, as shown in figure 2. A statistically significant 20–25% residual discrepancy with respect to P7CLEAN_V6MC remains above 10 GeV for both front and back events. Overall, we find that the new on-orbit PSF provides a good representation of the angular dispersion while preserving the dependence on the γ -ray incidence angle.

P7REP_V10 IRF tables are defined up to 1.8 TeV. However the energy reconstruction has been tested

¹<http://fermi.gsfc.nasa.gov/ssc/data/>

only up to 1 TeV. Therefore the FSSC data server will only release data up to 1 TeV by default. Users will be able to change the default query settings to access the events with energies above 1 TeV.

3. Validation and performance

Reprocessing data with up-to-date calibration constants provides us with a new data set that is significantly different from the one that we explored in the careful analysis published in Ackermann et al. [2012]. As soon the first P7REP data was available we started the low level verification (e.g., the characterization of the change in the energy scale). The validation process is still on-going at the highest level of science analysis, such as a full sky catalog-like analysis. We report here a few highlights.

3.1. Events switching event class

A first quantification of how reprocessed data are different is given by the fact that 25% of the events move from one class to another, as shown in figure 3 for the Source event class. This number was not unexpected, given the magnitude of the change in the CAL crystal light asymmetry calibration and its known impact on the tracking.

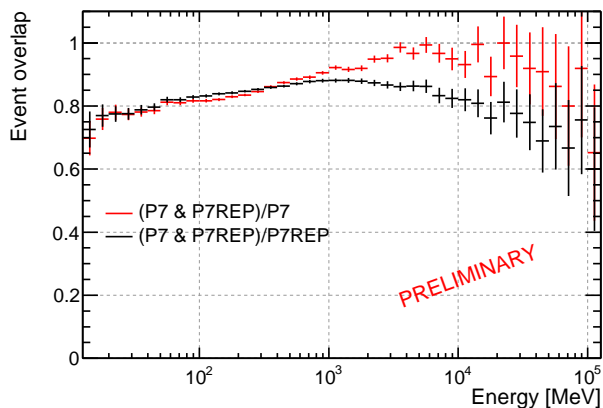


Figure 3: Relative overlap between P7REP_SOURCE and P7SOURCE. Up to 25% of the events move from one class to another.

3.2. Vela spectral analysis

Vela is useful as a reference because of its brightness, which makes the impact of the diffuse γ -ray backgrounds very limited on most types of analysis. Furthermore, we can use γ rays away from the pulse peaks to very effectively model the diffuse γ -ray backgrounds.

We analyzed both reprocessed and original data using the same procedure, which may be simply described as follows: we first fit one year of data in a large region around Vela, leaving all the parameters of the sources in the model free to vary. We then developed a model for the non-pulsed background near Vela using the sample of photons in a 10° region around Vela that are also away from the Vela phase peaks and that we fit using as input the parameters for the larger region. We then removed as spurious any sources that were not in the first Fermi source catalog Abdo et al. [2010]. We used this model as the background template for our phase-averaged analysis.

The model used to fit the Vela pulsar is a power-law with an exponential cutoff and is shown for both data sets in figure 4. Overall the results are roughly compatible in the sense that high level science is not radically changed, but statistically the reconstructed flux for P7REP_SOURCE data is higher by a few percent and the spectral index is slightly harder, confirming the impact of the reprocessing on the measurements performed with the LAT.

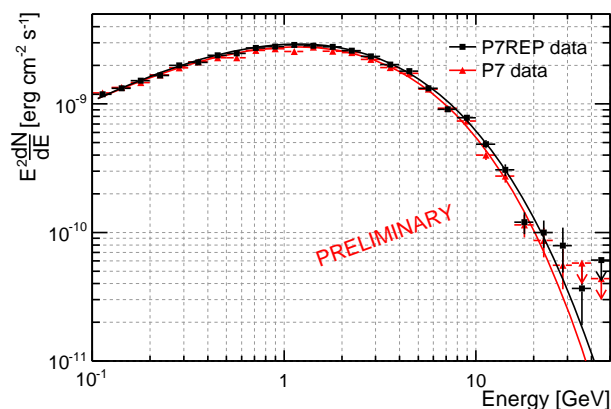


Figure 4: Phase-averaged spectrum of the Vela pulsar, measured with source class events using the first year of P7SOURCE and P7REP_SOURCE data.

3.3. Geminga flux stability

In order to check the stability of LAT data quality and data-analysis chain, we evaluated weekly binned light curves of the Vela and Geminga pulsars using a standard likelihood analysis. The resulting light curves are shown in figure 5 for the Geminga pulsar for 4 years of P7SOURCE and P7REP_SOURCE data. The flux in the P7REP_SOURCE data is again slightly higher ($\sim 2.7\%$) for both pulsars. In addition there is an increase in flux by $\sim 0.7\%$ per year detected for Geminga in the P7SOURCE data, which is not detected in the P7REP_SOURCE data for which the flux is stable within uncertainties over 4 years.

This result demonstrates that P7REP data are of better quality than P7 data, and have lower systematic uncertainties.

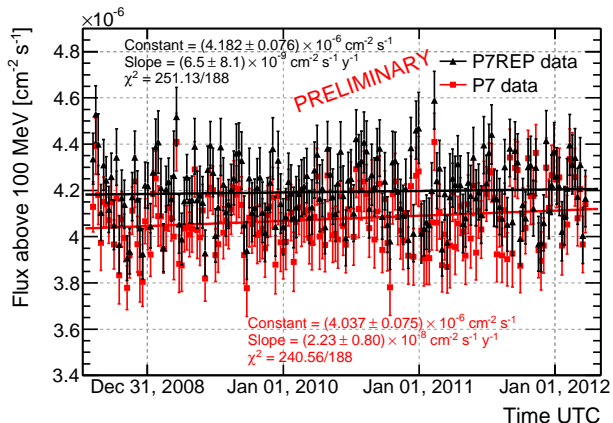


Figure 5: Long-term trending of the integral flux above 100 MeV for Geminga, measured using P7SOURCE and P7REP_SOURCE class events. Each data point represents a week's worth of data.

3.4. Hard-spectrum source list study

A preliminary higher-level test was provided by a comprehensive (re)analysis of ~ 1300 candidate hard sources that had a test statistics (TS) > 10 for 3 years of P7 data. We choose the harder sources for this analysis as they were more likely to be affected by improvements to the PSF at high energies. Again, both P7CLEAN and P7REP_CLEAN data sets between 10 and 500 GeV were analyzed in parallel. We note that the P7REP_CLEAN analysis used a preliminary version of the isotropic spectral template that was derived from the P7REP data.

There are 514 sources at $TS > 25$ in the P7CLEAN run, 561 with the P7REP_CLEAN data and 454 are in common. Again the relatively large number of sources not in common is to be expected, since P7REP data are really a new data set, and most of the sources in both lists are close to the TS threshold. Therefore small changes in TS can cause substantial changes in the source lists. The TS distributions for both data analysis runs are presented in figure 6. Overall the P7REP_CLEAN data give a slightly higher TS: on average the ratio P7CLEAN/P7REP_CLEAN is 0.82.

4. Conclusions

We have reprocessed *Fermi*-LAT data with up-to-date calibration constants, including a more accurate description of the position-dependent response of each CAL scintillator crystal and the slight decrease in scintillation light yield with time ($\sim 1\%$ per year) from

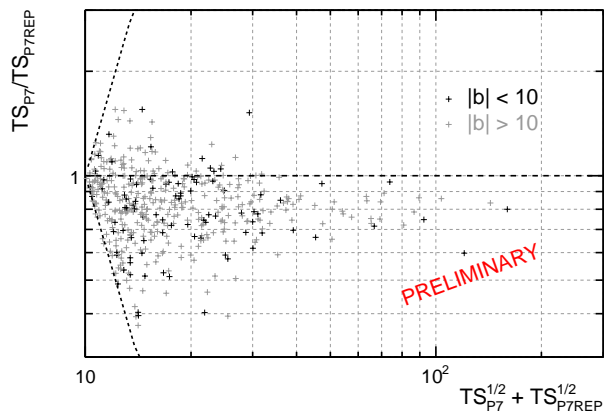


Figure 6: Ratio between the TS values obtained from the analysis of P7CLEAN- and P7REP_CLEAN-class events for a sample of candidate hard sources as a function of the sum of the detection significances.

radiation exposure on orbit. The main improvement to the instrument response is a narrower PSF core above a few GeV. For this reason, we have produced a new set of IRFs that include the new on-orbit PSF which is now based on a scaled version of the PSF derived from Monte Carlo simulations. The new IRFs also include a modification of the effective area, inferred from flux measurements using flight data, to correct symmetrically the front/back discrepancy in the effective area observed in the data.

Validation of the reprocessed data is ongoing within the collaboration and has already demonstrated an overall improvement in data quality, which has led to better standard source analysis. We expect to release these new data publicly through the FSSC in the spring of 2013. The main results shown in this paper will be updated to the final versions of the P7REP IRFs and made available through the FSSC as well.

Acknowledgments

The *Fermi* LAT Collaboration acknowledges support from a number of agencies and institutes for both development and the operation of the LAT as well as scientific data analysis. These include NASA and DOE in the United States, CEA/Irfu and IN2P3/CNRS in France, ASI and INFN in Italy, MEXT, KEK, and JAXA in Japan, and the K. A. Wallenberg Foundation, the Swedish Research Council and the National Space Board in Sweden. Additional support from INAF in Italy and CNES in France for science analysis during the operations phase is also gratefully acknowledged.

References

- A. A. Abdo, M. Ackermann, M. Ajello, J. Ampe, B. Anderson, W. B. Atwood, M. Axelsson, R. Bagagli, L. Baldini, J. Ballet, et al., *Astroparticle Physics* **32**, 193 (2009), 0904.2226.
- M. Ackermann, M. Ajello, A. Albert, A. Allafort, W. B. Atwood, M. Axelsson, L. Baldini, J. Ballet, G. Barbiellini, D. Bastieri, et al., *The Astrophysical Journal Supplement* **203**, 4 (2012), 1206.1896.
- S. Agostinelli et al. (GEANT4), *Nucl. Instrum. Meth.* **A506**, 250 (2003).
- A. A. Abdo, M. Ackermann, M. Ajello, A. Allafort, E. Antolini, W. B. Atwood, M. Axelsson, L. Baldini, J. Ballet, G. Barbiellini, et al., *The Astrophysical Journal Supplement* **188**, 405 (2010), 1002.2280.